Transient Response Study of Gas Flowing Through Irrigated Packing

FRANCESCO DeMARIA and ROBERT R. WHITE

University of Michigan, Ann Arbor, Michigan

The transient response of a gas phase as it flows through an irrigated packed column can be interpreted as a distribution of time spent by the elements of gas as they flow through the bed.

A step function in helium concentration was introduced in the entering air stream of a column packed with Raschig rings, and the outlet concentration was recorded with time. Water was used as the liquid phase. Size of Raschig rings, depth of bed, water and gas flow rates were the main variables investigated.

The response curve for the gas reveals an increasing departure from uniform flow of the gas stream as liquid and gas rates are increased to flooding. The first and second moments of the time distribution give directly the porosity and the axial dispersion of the gas. These quantities have been found to be mainly dependent on liquid flow rates. The skewness which characterizes the weight that the various gas elements have on the dispersion about the average residence time has been found to give a convenient measurement of the uniformity of gas flow through the bed.

Recently unsteady state experimental methods have gained increased attention in chemical engineering research because the time distribution characterizes the system and may also provide a similarity criterion in the scale up of equipment.

Unsteady state experiments are based on the measurements of the response of the system to a known disturbance in experimental conditions. Work of this type has already been reported for relatively simple process systems such as single-phase flow in pipes and packed beds (*2, 6, 8, 11, 13, 26*), reactors (*7, 14, 15, 29, 34*), and heat exchangers (*3*).

An unsteady state investigation of packed gas-liquid absorption equipment appeared to be both useful and interesting for the following reasons.

1. Simplified equipment such as wetted-wall columns and disk absorption columns yields data which are not easily applicable to predictions on the performance of packed absorbers (*5*). Mass transfer data obtained from experimental columns operated at steady state conditions appear to be in wide disagreement (*27*). These difficulties are apparently due to the fact that little is known about the flow of layers of liquid and gas over discontinuous surfaces. It is possible that information on the distribution of residence times of the gas and liquid streams flowing through the column may provide a satisfactory parameter for the correlation of absorption equipment performance.

2. Unsteady state experimental techniques applied to gas-liquid flow systems present unusual problems concerning the introduction of a predetermined disturbance in one of the entering phases and the separation of the effluent phase for rapid analysis; thus work of this nature has been scarce (*18, 21*).

The problem was limited to the study of the gas-phase response to a step function in tracer concentration in the inlet stream. Complicating effects such as absorption or chemical reaction between the liquid and gas streams were eliminated. The method of introduction of the transitory disturbance permitted the measurement of the column volume occupied by the gas and the degree of longitudinal mixing as function of gas and liquid flow rates and packing sizes.

Francesco DeMaria is with American Cyanamid Company, Stamford, Connecticut. R. R. White is now with Atlantic Refining Company, Philadelphia, Pennsylvania.

THEORY

The residence-time distribution is defined as the fraction of the entering feed flowing in the effluent per unit time which has been in the reactor between time, t, and $t + dt$. This quantity is usually indicated as $E(t)$. Danckwerts (*6*) has discussed in detail the manner in which the residence-time distribution can be determined from experiments in which the tracer is injected at the inlet either as an instantaneous pulse or as a step in its concentration.

Moments of the Residence-Time Distribution

The moments of the residence-time distribution are defined

$$\int_0^\infty t^n E(t)\,dt \qquad (1)$$

and may be used to characterize the time distribution. Table 1 lists the first four moments from the zero to the

third and the corresponding relationships in terms of the effluent concentration for a step input.

The zero moment is equal to unity since the sum of all fractions of feed over all times must be equal to one. (6).

The first moment of the residence-time distribution is equal to the mean age of the gas in the system, θ. As indicated in Table 1 this quantity is equal to the average residence time calculated as $\epsilon V/q$. van der Laan (32) and later Spalding (31) have indicated that whenever there is considerable diffusional transport across the inlet and/or outlet boundary the first moment will be greater than the average residence time $\epsilon V/q$. The excess of θ over $\epsilon V/q$ is a function of the longitudinal mixing occurring in the system. The first moment is primarily a function of the throughput and is relatively insensitive to longitudinal mixing.

The second moment about the mean residence time is a measure of the dispersion of the time distribution. This quantity shown in Table 1 has dimension of sec.^{2} and is indicated by the symbol S_θ^2. Levenspiel and Smith (23) call the dimensionless second central moment a *variance* and indicated it by the symbol σ^2.

In the type of experiments discussed here the signal is introduced in such a manner that the concentration normal to the direction of flow is uniform and the dispersion about the mean exhibited by the residence-time distribution is mainly caused by the longitudinal mixing taking place in the bed. It has been shown by Levenspiel and Smith (23) that for a model in which turbulent diffusion is responsible for this longitudinal mixing the variance is equal to

$$\sigma^2 = \frac{2E}{vL} + \frac{8E^2}{v^2L^2} \qquad (2)$$

so that when the dimensionless group vL/E is sufficiently large

$$\sigma^2 \cong \frac{2E}{vL} \qquad (3)$$

Another model visualizes packed beds as made up of a series of completely mixed cells. Klinkenberg and Sjenitzer (19) have shown that the dispersion in this case is

$$\sigma^2 = \frac{1}{n} \qquad (4)$$

The similarity between the turbulent-diffusion approach and the series of completely mixed stages model has been discussed by many authors (1, 2, 18, 19, 26) who have pointed out in various ways that for equivalence of the two models

$$n \cong \frac{vL}{2E} \qquad (5)$$

for large enough values of vL/E. This result is obtained by combining Equations (3) and (4) keeping in mind that (3) is only approximately correct for large values of vL/E (23, 32).

The first moment, being essentially equal to the average residence time $\epsilon V/q$, can be used to determine the void volume or the volumetric flow rate, whichever is unknown, or as a test of consistency for the experimental data. The second moment or the variance gives directly the effective diffusion coefficient or the number of perfectly mixed stages. In those cases in which the longitudinal mixing is large however these simplified relations may not hold. van der Laan suggests more appropriate methods of obtaining the longitudinal mixing parameter (32).

Deviations from Uniform Flow

In absence of any information on the actual velocity distribution in the column the dispersion of the time distribution, while giving a measure of the degree of longitudinal mixing, yields no information about the relative weight that the various fractions of feed have on the total dispersion. The third central moment of the distribution or the skewness defined in Table 1 may provide such additional information. For a series of perfectly mixed stages the skewness is $2/n^2$ when the flow through the bed is uniformly distributed. It follows therefore that the difference between the skewness and twice the square of the dispersion should be a measure of the degree of departure from uniform flow. Should this difference be large, neither turbulent diffusion nor the series of perfectly mixed stages would be satisfactory correlation models since they both assume uniform flow velocity across the bed.

End Effects

In the event that the experimental apparatus must include entrance and/or exit sections which cannot be conveniently isolated from the test section, the mixing introduced by such end effects can be expressed by well established statistical principles (4). The moments of the time distribution for each section of a system may be added if the statistical events taking place within each section are independent. Thus for the first moment of the distribution

$$\theta = \theta_1 + \theta_2 + \cdots + \theta_n \qquad (6)$$

For the second central moment

$$S^2_\theta = S^2_{\theta 1} + S^2_{\theta 2} + \cdots + S^2_{\theta n} \qquad (6a)$$

and for the variance

$$\sigma = \sigma^2_1 \frac{\theta^2_1}{\theta^2} + \sigma^2_2 \frac{\theta^2_2}{\theta^2} + \cdots + \sigma^2_n \frac{\theta^2_2}{\theta^2} \qquad (6b)$$

Klinkenber and Sjenitzer have given examples of this procedure (19). When considerable diffusional transport exists at the boundary between two sections of the system, independence of the statistical events taking place in each section should not be expected.

EXPERIMENTAL

The experimental apparatus was designed to introduce a signal of helium tracer in the inlet gas stream of an absorption column of suitable dimension and record the composition of the outlet continuously and with minimum delay. The equipment therefore consists of a gas and liquid supply, a packed test column, and a gas analyzer.

Flow System

Figure 1 shows a diagram of the equipment. Compressed air at 50 lb./sq. in. is humidified in a brass column 4 in. in diameter and 4 ft., 8 in. in height. The air rate is measured through a bank of three rotameters in parallel and is adjusted and maintained constant by a pressure regulator.

Pure helium or a mixture of 15% helium and 85% nitrogen are used as tracers. The tracer flow after a primary reduction in pressure is maintained at a constant rate by means of a second pressure regulator. A three-way solenoid valve immediately before the inlet to the test column permits replacing the air flow to the column with tracer or the introduction of a pulse of tracer as slugs of short duration in the air stream.

The test column is made out of 4-in. I.D. flanged Pyrex glass pipe. The bottom section of the column is conical, and a ¾-in. I.D. liquid outlet is located at the vertex of the cone. An adjustable liquid level device is used to maintain an adequate liquid seal to allow the outgoing liquid to disengage any gas bubbles before going to the drain. The total volume of the bottom section from the three-way solenoid valve to the beginning of the packing is 0.0065 cu. ft., and it constitutes 1.5 to 2% of the total volume of the column depending on the height of the mid-section.

The upper extremity of the column is reduced in diameter to 2-in. I.D. for connection with the gas analyzer. The liquid is introduced on a side inlet and is distributed by six jets made of 1-½-mm. capillary tubing evenly spaced on a 3-in. radius. The volume of the upper section is 0.0437 cu. ft. The mid-and upper-column sections are completely filled with packing up to the gas analysis cell. Thus a portion of packing which is in the upper section remains dry during the gas-liquid runs because it is above the liquid distributor.

The column is packed with Raschig rings of ¼-⅜-and ½-in. nominal diameter. The rings were made of unglazed porcelain.

Continuous Gas Analyzer

A continuous and accurate recording of the tracer concentration in the gas stream

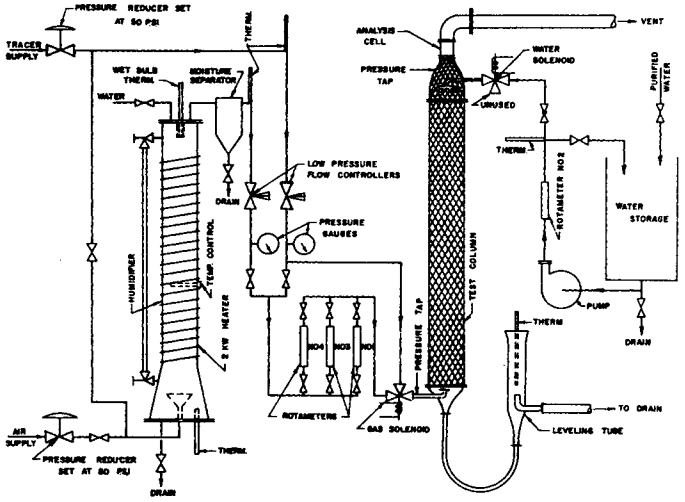

Fig. 1. Flow diagram.

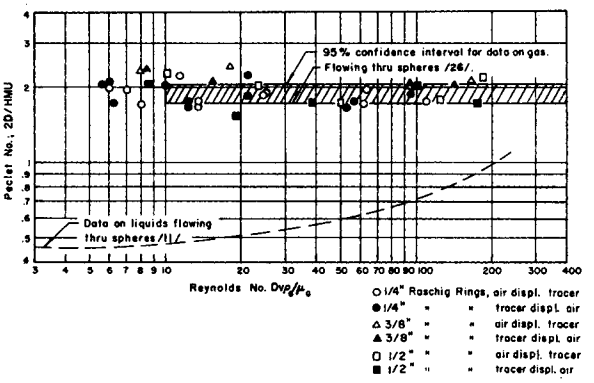

Fig. 3. Axial mixing through beds of spheres and Raschig rings (Peclet number vs. Reynolds number).

is obtained from an alpha particle ionization cell. Deisler, McHenry, and Wilhelm (9) used such analyzers for binary and ternary gas mixtures above atmospheric pressure. Details of the analyzer and recorder circuit are shown in Figure 2.

The electrodes of the cell are two rectangular stainless steel plates. The rectangular cell geometry was chosen to give most favorable current stability and noise characteristics. When one uses pure helium as the tracer, the output is exceedingly stable and free of stray noise. The plate used as the alpha particle emitter has on one side an active area of 1⅛-in. by 1⅛-in. covered with 100 μg. of radium 266 rolled in gold foil. The other plate is the ion collector. The plates are spaced at a distance of 1 in. within a 2-in. O.D. Teflon mount especially streamlined to minimize extraneous mixing of the gas entering the cell. The assembly is housed in a specially fabricated glass-flanged tube 3 in. long which is inserted between two 2-in. Pyrex brand pipe flanges forming the connection between the top of the test column and the exhaust pipe. The glass housing and the high impedance leads are shielded with brass foil.

A potential of about 1,000 v. across the electrodes is necessary to collect all the ions formed by the alpha particles. Thus this voltage was selected as standard throughout the experimental work. The output current of the electrodes at 1,000 v. potential varies linearly with helium concentration from a value of 1.9×10^{-8} amp. for pure helium to 9.1×10^{-8} for air.

The low output current from the electrodes is boosted by a 187 megohm resistor across the ion collector plate and the ground to a maximum potential drop of 17 v. To allow the use of 15% helium 85% nitrogen mixture as a tracer a current blocking circuit is inserted in series with the resistor. This consists of a 15-v. mercury battery connected with inverted polarity so that this constant voltage is subtracted from the high resistance circuit; the maximum output voltage corresponding to 100% air is 2 v. The high sensitivity circuit causes a certain amount of noise to be detected in the cell output; thus a 250$\mu\mu$ farad capacitor was added across the high sensitivity circuit to damp some of it out.

The increased capacitance of the high sensitivity circuit resulted in an increase in the time constant of the analyzer recorder system from 0.005 to 0.05 sec. In the experiments performed the average residence time varied from about 4 to 80 sec.; thus the lag of the analyzer recorder system was ignored since it constituted in most cases less than 1% of the total time lag.

Preliminary Tests

The manner of introduction of the tracer at the column inlet was soon limited to step changes in concentration since it was found impossible to inject an appreciable amount of tracer in a short interval of time, as compared with the contact time of the gas flowing through the column, in order to approximate an impulse signal.

Pure helium was first used as a tracer in preliminary work. It was found however that when the helium displaced the air through the column, the response curves were severely distorted especially at low flow rates. This phenomenon was attributed to the presence of convective currents due to the difference in density of the two gases.

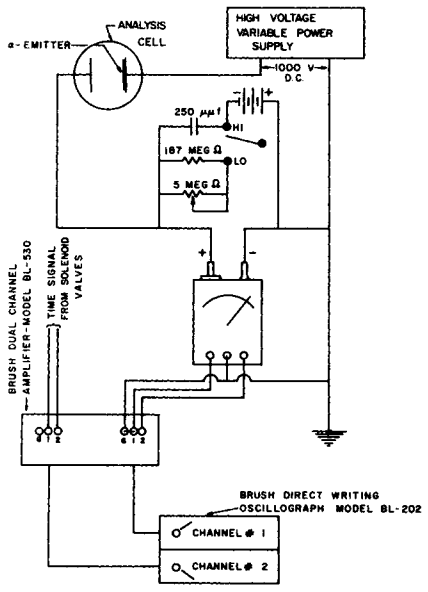

Fig. 2. Assembly of gas analyzer and accessories.

Most of the experimental work used as tracer a mixture of 15 volumes of helium and 85 volumes of nitrogen. The difference in density with air is about 16%, and the resulting response curves for the tracer displacing the air and for the air displacing the tracer were in reasonable agreement.

Standard Experimental Technique

Raschig rings of the desired size were introduced into the column by partially filling the column with water, then slowly pouring the rings from the top. The water prevented breakage and provided slow and even settling of the rings.

The porosity of the dry bed was determined by back filling the column with a known amount of water and measuring the resulting increase in liquid level.

For an irrigated packing run the packing was first thoroughly wetted by adjusting the water rate to 6,000 lb./hr./sq. ft. for about 1 hour. Then a series of runs was performed by adjusting the liquid and gas flows to the desired rates. For each liquid flow rate the column was allowed to reach equilibrium for about a half-hour. Then response curves were recorded at 15-min. intervals and compared by superposition to note if the curves were exactly congruent. If not the gas and liquid flow rates were checked and the procedure repeated until two successive sets of curves were in agreement. When flooding was reached, the flow conditions through the column were too erratic to obtain consistent response curves so that no data was obtained on or about this range of conditions. Only for run W-19 was a reasonable agreement for successive response curves obtained even though the column was flooded. The dynamic liquid holdup was measured at the end of some of the irrigated packing runs by interrupting simultaneously the gas and liquid flow and collecting the total amount of liquid drained from the column.

When a series of runs was completed and a change over of packing was neces-

Table 1. Quantities Characterizing a System in Terms of its Transient Response

Moments of the distribution of residence-times function $E(t)$		Relationships in terms of outflow concentration: Step input from 0 to C_o	Relationships in terms of outflow concentration: Impulse input (amount Q of tracer injected instantaneously)
Zero moment of $E(t)$ vs. t	$\int_o^\infty E(t)dt = 1$	$\int_o^\infty dc/C_o = 1$	$\int_o^\infty cdt = \frac{Q}{v}$
About $t = 0$ axis First moment of $E(t)$ vs. t	$\int_o^\infty tE(t)dt = \theta \simeq \frac{\epsilon V^*}{v}$	$\int_o^\infty (1-c/C_o)dt = \theta \simeq \frac{\epsilon V}{v}$	$\frac{v}{Q}\int_o^\infty tcdt = \theta \simeq \frac{\epsilon V}{v}$
About $t = 0$ axis Dispersion, second moment of $\theta E(t)$ vs. t/θ	$\sigma^2 = \int_o^\infty (t/\theta)^2\theta E(t)d(t/\theta) - 1$	$\sigma^2 = \frac{2\int_o^\infty t(1-c/C_o)dt}{\theta^2} - 1$	$\sigma^2 = \frac{\left(\frac{v}{Q}\right)^2\int_o^\infty t^2cdt}{\theta^2} - 1$
About $t/\theta = 1$ axis Skewness, third moment of $\theta E(t)$ vs. t/θ	$\nu = \int_o^\infty (t/\theta)^3\theta E(t)d(t/\theta)$	$\nu = \frac{3\int_o^\infty t^2(1-c/C_o)dt}{\theta^3}$	$\nu = \frac{\left(\frac{v}{Q}\right)^3\int_o^\infty t^2cdt}{\theta^3}$
About $t/\theta = 1$ axis	$-3\int_o^\infty (t/\theta)^2\theta E(t)d(t/\theta) + 2$	$-\frac{6\int_o^\infty t(1-c/C_o)dt}{\theta^2} + 2$	$-\frac{3\left(\frac{v}{Q}\right)^2\int_o^\infty t^2cdt}{\theta^2} + 2$

* This relationship holds only in those cases where transfer of mass at the inlet and outlet boundaries is negligible.

sary, the porosity was again checked. Then the packing was removed and weighed in such a manner as to determine the total number of particles.

RESULTS AND DISCUSSION

Dry Packing

The experimental effort was first directed to the study of the gas phase mixing through the bed in order to verify the suitability of the equipment and the method of analysis against existing data.

Consistency Checks. The consistency of the gas holdup information furnished by the transient response curve was checked by comparing θ with the average residence time computed from the known void volume and gas flow rates. For the twenty-three experiments performed (*10*) the agreement between these two quantities was found to be within ± 8%. The random deviation could be easily accounted for by considering the precision of the rotameter calibration, the reading of the recorder traces, and the subsequent handling of the data by graphical integration. It was thus concluded that for the system under study the mean age θ was for practical purposes equal to the residence time.

In accordance with the correlation models discussed previously the variance is equal to the reciprocal of the number of perfectly mixed stages in series or approximately equal to $2E/vL$. The latter quantity was estimated independently by superimposing a graph of c/C_o vs. t/θ as obtained from a given recorder trace over previously prepared graphs for the infinite column solution of the diffusion equation with increments of the group $vL/2E$ of ten units from $vL/2E = 80$ to $vL/2E = 200$. The variance and the group $2E/vL$ were found in all cases within 10% in good agreement with the theory, and Equation (5) was considered adequate for the purpose of this data analysis. Because the variance as calculated from the response curves was believed more accurate than the estimation of the group $vL/2E$, it was decided to adopt the number of mixing stages or the inverse of the variance as a measure of the extent of mixing taking place in the column.

Considerable attention was given to end effects introduced by entrance and exit sections to the test column. The correlation model, in which the packed bed is considered as made up of a series of perfectly mixed stages, gives the height of a mixed stage:

$$HMU = \frac{L}{n} \qquad (7)$$

Accordingly two bed heights 3 and 4 ft. were investigated to ascertain the presence of end effects. The average of all runs for the shorter bed gives a height of a mixed stage of 0.0247 ft. as compared with 0.0228 ft. for the longer bed.

On the assumption that the empty entrance section is equivalent to a perfectly mixed stage, the calculated variance was corrected by subtraction of the empty section contribution to the total variance in accordance with Equation (6*b*). After correction the average bed heights are 0.0228 and 0.0214 for the shorter and longer bed, respectively.

Consequently while the height of a mixed stage for the two bed lengths before correction differs by 8%, the difference is only 6% after the end correction is applied. This type of behavior is expected if the correction is real. On this basis it is presumed that the height of a mixed stage can be considered independent of column height.

It should be noted that no attempt was made to determine the actual degree of mixing taking place in the entrance section. The assumption that this section corresponds to one complete mixer leads to the largest possible correction, and as seen above this is quite small and within the precision of the data.

It may be seen from Figure 1 that the exit section varies in diameter from 4 down to 2 in. In order to take this fact into account an effective column

Table 2. Characteristic Lengths for Peclet Number Correlation

Nominal particle diameter, in.	Particle to bed diameter ratio, D/D_t	Number of runs with random packing	Mean Peclet number $NPe = \frac{2D}{HMU}$	$NPe' = \frac{2D_p}{HMU}$	$NPe'' = \frac{2D_m}{HMU}$
¼	0.0625	22	1.87	1.73	0.331
⅜	0.0938	8	2.18	2.04	0.357
½	0.1250	10	1.89	1.82	0.335
Mean value of above numbers			1.98	1.86	0.340
Mean square deviation			0.03006	0.02543	0.00043

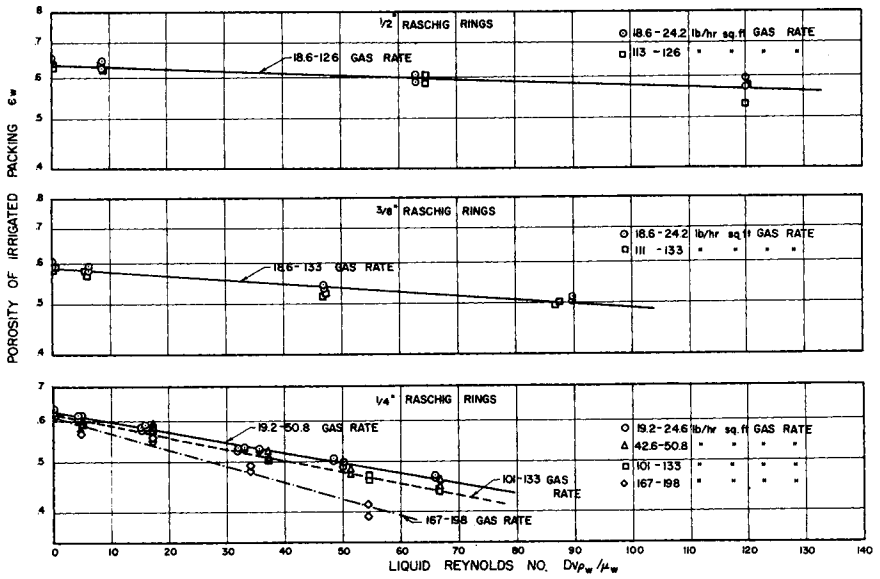

Fig. 4. Effect of liquid flow rate on porosity of irrigated packing.

length was used in the calculation of the height of a mixed stage. This was taken equal to the total volume of the equipment divided by the nominal column diameter (4 in.). To verify that this assumption was correct, runs were made with the upper section left empty and without distributor or completely filled with packing. The height of the mixed stage, computed by the use of the actual length of the test section in the first case and the effective column length in the latter case, was found in good agreement.

Comparison with Previous Investigators. An extensive study of axial mixing for gases flowing through packed beds of spheres is reported by McHenry and Wilhelm (*26*), who used a frequency-response technique. The data of these authors is represented in Figure 3 as a shaded band indicating the 95% confidence limits for the Peclet number. The data for the Raschig rings as obtained in the present work are also shown in Figure 3. The Peclet number is calculated as the ratio of twice the nominal particle diameter to the height of a perfectly mixed stage, and it is analogous to the Peclet number used by McHenry and Wilhelm except that the nominal ring diameter is used in place of the diameter of spheres. The gross agreement between the two sets of data as shown by Figure 3 may be quite fortuitous because clearly there is little hydrodynamic relationship between Raschig rings and spheres having the same diameter. However this figure serves to point out that the Peclet number is of the same order of magnitude in both sets of experimental data for both techniques of signal input, that is step-function response and frequency response.

An analogous conclusion was also obtained by Ebach (*11*) who has extensively studied axial mixing of liquids through packed beds of spheres and other packing shapes. The dotted line in the lower region of Figure 3 is representative of data obtained in his experiments with two types of unsteady state techniques, that is transient and frequency response. Other data for liquids obtained by Danckwerts (*6*) and Kramers and Alberda (*18*) also fall in the neighborhood of the dotted line.

A statistical analysis of the data obtained on Raschig rings shows that a least squares straight line through the points plotted on Figure 3 has no significant slope. Thus no apparent effect of Reynolds number in the investigated range is detectable. Therefore the Peclet number can be expressed as the true mean of forty points and is found to be equal to 1.94 ± 0.07. In statistical language the foregoing can be expressed as:

$$Pr\ (2.01 > N\,Pe > 1.87) = 95\% \quad (8)$$

These results compare well with those of McHenry and Wilhelm.

Effect of Particle Diameter. In the preceding paragraph it was tacitly assumed that the Peclet number computed as the ratio of the nominal Raschig ring diameter to the height of the mixing stage was independent of particle diameter. However this dimension is seldom used to characterize Raschig rings. More frequently the equivalent spherical diameter D_p is used (*22*). Ebach (*11*) employed this quantity in the study of axial mixing of liquid flowing through a bed of Raschig rings. For pressure drop through granular beds Kozeny (*20*) suggested as hydraulic mean diameter the quantity

$$D_m = \frac{\epsilon}{(1-\epsilon)S} = \frac{\epsilon}{a} \quad (9)$$

For spheres this quantity is

$$D_m = \frac{\epsilon D}{6(1-\epsilon)} \quad (10)$$

Since the porosity for a packed bed of spheres varies about a value of 0.4, the value of D_m is approximately 1/10 of the actual diameter of the sphere.

Table 2 was prepared to compare the suitability of each of these quantities in the correlation of the data.

On the basis of the foregoing results it is apparent that the hydraulic mean diameter is the best correlation parameter for the effect of particle size and porosity on Peclet number.

It should be noted that no attempt was made to study experimentally the hydrodynamic relationship between Raschig rings and other shapes such as spheres. No universal simple relation exists among all shapes to a common characteristic length. As the result of this work Kozeny's hydraulic mean diameter would appear to be a more general characteristic length than the nominal particle diameter. This quantity however is also a function of the packing porosity which varies according to the method of packing or with liquid and gas flow rates in the irrigated runs. For this reason the nominal diameter of the rings was preferred in the calculation of the Reynolds number which is used as the independent variable.

Irrigated Packing

Wet Porosity. The porosity of the wet packing and the extent of mixing

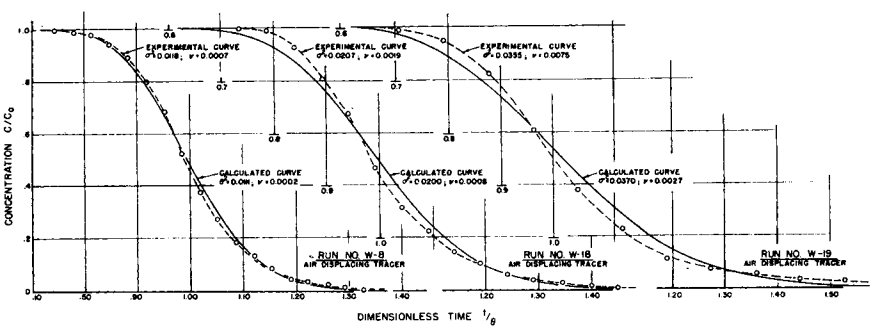

Fig. 5. Response curves showing departure from uniform flow.

taking place in the gas stream were measured in a series of forty-two runs (*10*). The variables investigated were gas and liquid flow rates and diameter of Raschig rings.

Dry-packing experiments served to verify that the mean age, as obtained from recorded concentration-time curves, can be used to calculate the volume of the bed occupied by the gas. On this basis the porosity of the irrigated bed for which no other method of direct measurement is presently known is calculated from a knowledge of the mean age of the gas θ and the corresponding volumetric flow rate. The data is shown graphically in Figure 4, where the wet porosity is plotted vs. the Reynolds number of the liquid. It can be seen here that the liquid rate is the most important variable and that the relationship between the liquid rate and the porosity is exponential in the liquid Reynolds number. Accordingly the equation

$$\frac{\epsilon_W}{\epsilon} = 0.90 \times 10^{-3.43 \times 10^{-6}\left(\frac{D}{D_t}\right)^{2.31} N_{Re_w}} \tag{11}$$

was found to correlate the data. The statistical details of the correlation and confidence interval of the constants used in Equation (11) are reported elsewhere (*10*).

The intercept ϵ_{wo} of the wet porosity vs. liquid Reynolds number plot (Figure 4) represents the porosity of the wet packing at zero liquid flow rate; thus the difference $\epsilon_{wo} - \epsilon_w$ should correspond to the dynamic holdup. This quantity was found to be in good agreement with the amount of liquid drained from the column where both liquid and gas rates were suddenly interrupted in nine runs with ¼-in. packing (*10*). The values of $\epsilon_{wo} - \epsilon_w$ for ⅜- and ½-in. rings are also in fair agreement with operating holdup data of Shulman, Ullrich, and Wells (*30*) and Jesser and Elgin (*17*) considering slightly different packing dimensions,

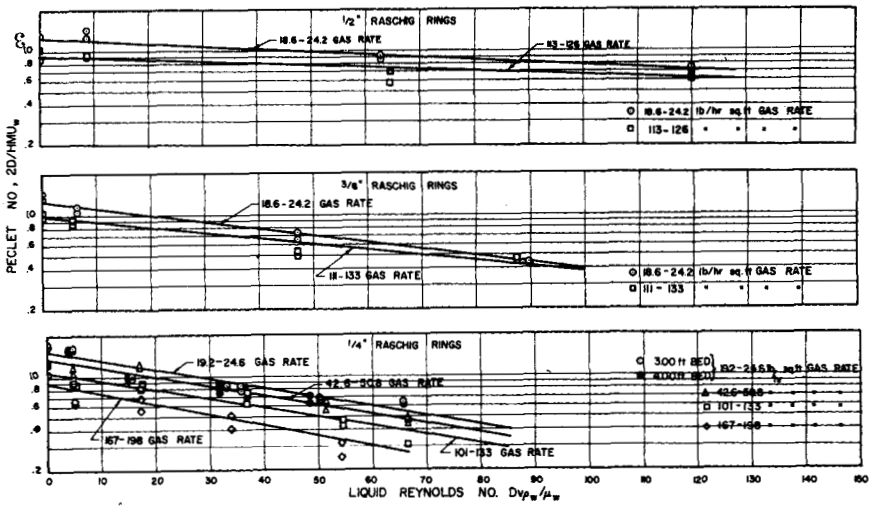

Fig. 6. Effect of liquid flow rate on Peclet number for irrigated packing (Peclet number vs. liquid Reynolds number).

differences in porosities of the dry packing, and differences in drainage time.

End Effects and Departure from Uniform Flow. For the irrigated packing experiments the packed test column was made up of three portions: a bottom empty entrance section, an irrigated section, and a section remaining dry above the liquid distributor. Again, it is assumed that the bottom section is equivalent to a complete mixer. The number of mixed stages contributed by the dry section of packing above the liquid distributor is estimated from the results of previous experiments on dry packing. The significance of the correction as applied to the variance is best understood when data on beds of different depths are compared; this is done in Table 3 where data obtained from ¼-in. Raschig ring beds having irrigated depths of 3 and 4 ft. are compared under similar operating conditions. For each run the height of a perfectly mixed stage as calculated from the variance before and after correction is reported. A more satisfactory agreement is obtained after the correction is applied. The end effects appear to be adequately accounted for on this basis, and the bed depth is no longer considered as a pertinent variable.

In the study of the gas mixing through the irrigated packing it was noted that as the liquid and gas flow rates were increased, the response of the system could no longer be correlated in terms of any of the models discussed in the theory in which uniformity of flow is assumed.

As previously suggested the difference between the skewness and twice the square of the variance was assumed to be a measure of the degree of departure from uniform flow or channeling. Figure 5 gives a graphical presentation of the distortion in the response curves by comparing a theoretical curve for which the quantity $\nu - 2\sigma^2$ is zero with an experimental curve having the same variance, but for which $\nu - 2\sigma^2$ is increasingly important.

The magnitude of the deviation from uniform flow was found to be somewhat erratic (*10*). Although this is partly due to the difference of two

TABLE 3. EFFECT OF IRRIGATED BED DEPTH ON LONGITUDINAL MIXING

					Air displacing tracer				Tracer displacing air			
Run number	Nominal packing diameter, in.	Depth of irrigated packing, ft.	Liquid flow rate, lb./hr. sq. ft.	Air flow rate, lb./hr. sq. ft.	Calculated dispersion	Height of mixed stage (uncorrected)	Corrected dispersion	Height of mixed stage (corrected)	Tracer flow rate, lb./hr. sq. ft.	Calculated dispersion	Height of mixed stage (uncorrected)	Corrected dispersion	Height of mixed stage (corrected)
W-4	¼	3	446	23.6	0.00793	0.0238	0.00854	0.0256	20.2	0.00803	0.0241	0.00869	0.0261
W-23	¼	4	447	24.2	0.00612	0.0245	0.00650	0.0260	19.3	0.00620	0.0248	0.00659	0.0264
W-1	¼	3	1,600	24.0	0.01144	0.0343	0.01383	0.0415	24.6	0.01199	0.0360	0.01466	0.0440
W-24	¼	4	1,600	24.2	0.00896	0.0358	0.01038	0.0415	19.3	0.00950	0.0380	0.01113	0.0445
W-2	¼	3	3,340	24.0	0.01330	0.0399	0.01670	0.0501	24.6	0.01324	0.0397	0.01659	0.0498
W-25	¼	4	3,340	24.2	0.01133	0.0453	0.01372	0.0549	19.3	0.00999	0.0400	0.01179	0.0472
W-3	¼	3	5,070	24.0	0.01625	0.0488	0.02156	0.0647	24.6	0.01581	0.04743	0.02080	0.0624
W-26	¼	4	5,070	24.2	0.01357	0.0543	0.01701	0.0680	19.3	0.01193	0.0477	0.01462	0.0585

TABLE 4. COEFFICIENTS FOR MIXING CORRELATION

Run number	Nominal particle diameter, in.	Range of liquid flow rates, lb./hr. sq. ft.	Average gas Reynolds number	Total number of points	NPe_{wo}	95% confidence interval	M	95% confidence interval
W-1 through W-7	¼	0-6,190	19.2-24.0	14	1.528	±0.030	0.0069	±0.0013
W-23 through W-26	¼	447-5,070	19.3-24.2	8	1.500	±0.064	0.0079	±0.0038
W-8, W-11, W-14, W-17 and W-20	¼	446-6,190	42.6-50.8	10	1.334	±0.038	0.0068	±0.0017
W-9, W-12, W-15, W-18, W-21, W-22	¼	0-6,190	101-133	12	1.072	±0.035	0.0067	±0.0014
W-10, W-13, W-16, W-19	¼	446-5,050	167-198	8	0.895	±0.053	0.0079	±0.0027
W-27 through W-30	⅜	0-6,200	18.6-24.2	8	1.265	±0.032	0.0053	±0.0009
W-31 through W-34	⅜	0-6,200	111-133	8	0.979	±0.045	0.0041	±0.0013
W-35 through W-38	½	0-6,200	18.6-24.2	8	1.254	±0.021	0.0020	±0.0004
W-38 through W-42	½	0-6,200	113-126	8	0.928	±0.060	0.0014	±0.0012

numbers σ^2 and ν of the same order of magnitude and subject to inaccuracy in their numerical evaluation, it is evident that the departure from uniform flow may fluctuate greatly for any one run as indicated by random variations for the same experiment when different run records are compared. Departure from uniform flow appears to be most affected by an increase in liquid flow rates. Gas flow rates appear also to have an effect, but while this is not detectable for liquid loadings below 3,000 lb./hr./sq. ft., it becomes more pronounced above this flow and is greatest when flooding is observed.

The above qualitative information gives some indication that the distortion in the response curve is perhaps due to the random occlusion of the gas flow channels by the liquid resulting in maldistribution of the gas through the bed. Consistent with this hypothesis the departure from uniform flow would increase with liquid flow rates until a point is reached in which the liquid forms a continuous phase throughout the bed (flooding). When this occurs, the gas is compelled to lift the liquid from the pores in a pulsating manner and will proceed through the column in the form of bubbles rather than a continuous stream. Consequently uniformity of gas distribution can hardly be expected.

Axial Mixing Correlation. In a manner analogous to the previous correlation for mixing of the gas through the dry packing, the axial mixing was expressed in terms of the Peclet number defined as the ratio of twice the nominal particle diameter to the height of a mixed stage.

The data in question are shown in Figure 6, where the Peclet number is plotted vs. the Reynolds number of the liquid at constant gas rate for all three different packing sizes investigated. The lines drawn through the points are calculated by the least-squares method in accordance with

$$NPe_w = NPe_{wo}\, 10^{-MNRe_w} \qquad (12)$$

The constants NPe_{wo} and M were evaluated separately for nine groups of runs during each of which the bed properties, that is particle diameter and bed porosity, were the same, and the gas flow rate varied over a narrow range so that its effect could be assumed negligible. Table 4 gives a list of the constants and the groups of runs for which they were evaluated. A statistical test shows that the average value of M for all runs having the same particle size is no different from the least squares value for individual groups of runs reported on Table 4. It can also be shown that the constants M and NPe_{wo} are power functions of the particle diameter and the gas Reynolds number, respectively (*10*).

From the foregoing the data can thus be represented by

$$NPe_w = 2.4(NRe_G)^{-0.20} \times 10^{-\left(0.013-0.088\frac{D}{D_t}\right)N_{Re_w}} \qquad (13)$$

Equation (13) can also be written in terms of the height of perfectly mixed stages:

$$HMU_w = 0.83(NRe_G)^{0.20} \times 10^{\left(0.013-0.088\frac{D}{D_t}\right)N_{Re_w}} \qquad (13a)$$

Interpretation of Mixing Data. If one uses the series of perfectly mixed stages model to interpret the results pertaining to the mixing taking place in the bed, one observes that the height of a mixed stage is smaller for dry packing than it is for wet packing. Since the height of a mixed stage is as seen in the dry packing correlation, proportional to the particle diameter, one may postulate that as the liquid descends on the packing, it envelops several packing elements to form larger aggregates thus increasing the apparent diameter of the particles, or in an equivalent manner increasing the height of a mixed stage. Consistent with this interpretation Equation (13*a*) shows that HMU increases with liquid flow rate.

An idea of the validity range of Equation (13) is given by Figure 7, where the average Peclet number for dry Raschig rings is compared with data on irrigated packing. The line for wet packing calculated from Equation (13) for a liquid flow rate equal to zero is representative of all three packing sizes used in the experiments. It is apparent that Equation (13) cannot be used to extrapolate mixing data for Reynolds numbers much less than 10 since from the preceding remarks one would expect the Peclet number for wet packing to remain always below that for dry packing. The lower line shows ¼-in. packing data for a liquid flow rate from 5,050 to 5,070 lb./hr./sq. ft. The points on the extreme right of this line are for run W-19 which was conducted under flooding conditions. Equation (13) yields higher values of the Peclet number than those observed.

A more interesting but highly speculative interpretation of the Peclet number may be given on the assumption that the ratio of hydraulic mean diameter to height of a mixed stage is a constant. As seen from Table 2 this is quite true generally for dry packing. One may assume therefore that

$$NPe'' = NPe''_w = \frac{2\frac{\epsilon}{\theta}}{HMU} = \frac{2\frac{\epsilon_w}{\theta_w}}{HMU_w} = \text{Constant}$$

Accordingly by dividing Equation (13*a*) by HMU as given by Equation (8) one finds that

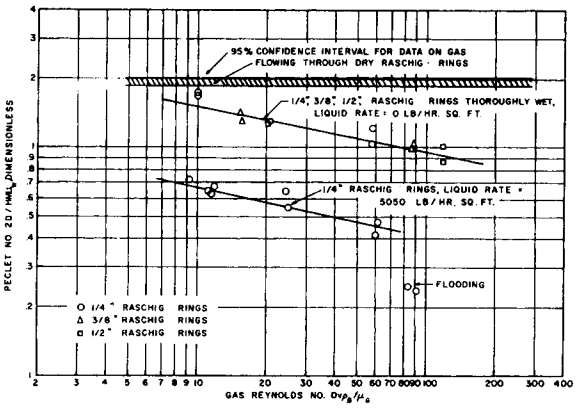

Fig. 7. Longitudinal mixing for gas flowing through irrigated beds of Raschig rings.

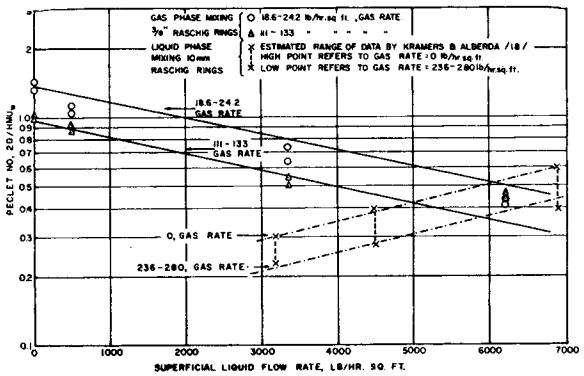

Fig. 9. Peclet number for liquid and gas phase flowing countercurrently through a packed bed of Raschig rings.

$$\frac{HMU_w}{HMU} = \frac{a\epsilon_w}{a_w\epsilon} = 0.81(NRe_G)^{0.20}\, 10^{\left(0.013-0.088\frac{D}{D_t}\right)N_{Re_w}} \qquad (14)$$

so that the ratio of total wet packing area to dry area is obtained by dividing Equation (11) by (14):

$$\frac{a_w}{a} = 1.11(NRe_G)^{-0.20} \cdot 10^{-\left[0.013-0.088\frac{D}{D_t}-3.43\cdot10^{-6}\left(\frac{D}{D_t}\right)^{-2.31}\right]N_{Re_w}} \qquad (15)$$

Equation (15) indicates that the wetted area would decrease rapidly with liquid flow rate and at a faster rate in fact than the porosity of the wet packing. In addition the rate of decrease in area is much more pronounced for the smaller size packing than it is for larger sizes. The wetted area could also be affected but to a lesser extent, by the gas Reynolds number. This may be due to the fact that higher gas flow rates tend to make the liquid-packing aggregate more compact so that it presents less surface area to gas flow. The cumulative result of these effects is to reduce the wetted-surface area in inverse proportion to the particle size so that the area of the packed bed exposed to gas flow may, at high liquid flow rates, be larger for larger packing sizes than for the smaller packing. Figure 8 shows the relationship between the total area of the bed in contact with flowing gas as estimated by Equation (15) together with estimates of effective mass transfer area (*12, 25, 33*). The uncertainty of data on effective mass transfer area is illustrated by the low and high values reported for ½-in. Raschig rings. The data of Mayo, Hunter, and Nash (*25*) obtained by measuring the colored surface area of Raschig rings made of paper over which water containing a red dye was circulated appear in line with the total surface area as given by Equation (15). In fact one would expect that the mass transfer area is only a fraction of the total surface area exposed to gas flow and that the former increases with increasing liquid flow rates so that the two quantities approach each other asympototically.

It is possible that the area which the bed presents to liquid flow is more directly related to the effective mass transfer area. If the reasoning followed in the derivation of Equation (15) is valid, (this could be verified by obtaining mixing data on other packing shapes) then the surface area which the bed presents to gas flow could be evaluated by a study analogous to the present one for the liquid phase.

Comparison with Previous Investigators. In connection with the previous discussion it is interesting to compare the present data on the gas-phase mixing with the results reported in graphical form by Kramers and Alberda (*18*) on a number of experiments in which the mixing of water running over 10-mm. Raschig rings in an absorption column with a countercurrent air flow was measured by frequency response.

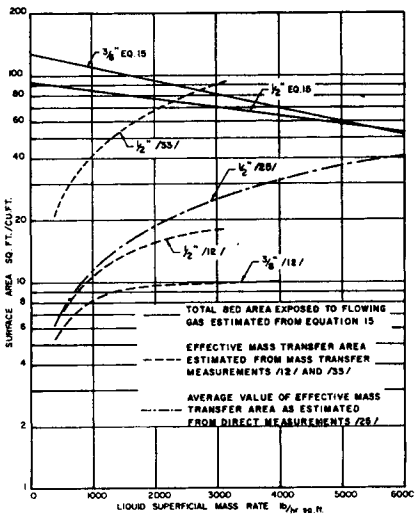

Fig. 8. Total bed area exposed to flowing gas and effective mass transfer area as function of liquid flow rate.

Figure 9 shows the Peclet number for the gas as measured in the present work for ⅜-in. rings (closest dimension to 10 mm.) with analogous Peclet numbers for the liquid as estimated roughly from the graphical data reported by the above authors. It is apparent from this figure that while mixing in the gas phase increases both with liquid and gas rates, in the liquid phase instead, mixing decreases with increasing liquid rates. The results on the liquid phase have to be accepted with some reservation because of their scarcity and because Kramers and Alberda do not give details about the experimental technique used. However they seem to show that according to the discussion of the previous paragraph the area which the bed presents to the flow of liquid does, indeed, behave in a similar manner to the effective mass transfer area.

Another interesting aspect of this comparison is that according to Figure 9 the Peclet number or the height of the mixing stage for both phases is of the same order of magnitude in the practical range of liquid flow rates. This fact may have some importance in greatly simplifying the interpretation of mass transfer data.

CONCLUSIONS

The residence time distribution study presented here suggests new possibilities concerning the mechanism of gas flow through Raschig rings irrigated by liquid.

Recent methods of analysis of transient experiments (*19, 23, 32*) have been employed to correlate the data. The moments of the residence-time

distribution have in themselves a physical meaning which is not necessarily associated with a predetermined physical model.

A correlation of the first moment of the time distribution shows that the porosity of the wet packing is primarily a function of the liquid flow rate, the dry packing porosity, and the nominal packing diameter.

The variance of the residence-time distribution clearly indicates that the axial dispersion of the gas flowing through the irrigated packing is markedly greater than that for the dry packing.

The extent of mixing expressed in terms of the Peclet number appears to be a function of the following variables in order of decreasing importance: liquid flow rate, nominal diameter of the packing, and gas flow rate.

The skewness of the residence-time distribution indicates that one-dimensional diffusion models and series of perfectly mixed stages are acceptable representations of the gas flow through dry columns having packed lengths large in comparison to the nominal diameter of the packing elements. For irrigated packing instead such models appear inadequate because the flow through the column is not uniform, especially when the flooding region is approached.

On the assumption that the Peclet number for single-phase flow is a constant over a discrete range of flow rates, the area of the packing exposed to gas flow can be determined. This information may be of use in the interpretation and correlation of mass transfer data.

NOTATION

A = cross-sectional area of empty column, sq. ft.

a = total surface area of bed, sq. ft./cu. ft.

a_w = total surface area of irrigated bed, sq. ft./cu. ft.

c = tracer concentration in effluent at time t, moles/unit vol.

C_o = tracer concentration in entering stream, moles/unit vol.

$E(t)$ = distribution of residence-time function, sec.

E = effective diffusivity in the direction parallel to flow in packed bed, sq. ft./sec.

D = nominal diameter of packing element, ft.

D_m = hydraulic mean diameter ϵ/a, ft.

D_p = diameter of sphere having equal volume as packing element, ft.

D_t = diameter of packed column, ft.

HMU = height of a perfectly mixed stage L/n, ft.

HMU_w = height of a perfectly mixed stage for irrigated bed, ft.

L = length of packed bed, ft.

M = coefficient for mixing correlation for irrigated packing, dimensionless

n = number of perfectly mixed cells in series in longitudinal direction

NPe = longitudinal Peclet number, Dv/E or $2D/HMU$, dimensionless

NPe' = modified longitudinal Peclet number, $D_p v/E$, dimensionless

NPe'' = modified longitudinal Peclet number, $D_m v/E$, dimensionless

NPe_w = longitudinal Peclet number for irrigated packing, $2D/HMU_w$, dimensionless

NPe_w'' = modified longitudinal Peclet number for irrigated packing, $2D_m/HMU_w$, dimensionless

NPe_{wo} = coefficient for mixing correlation for irrigated packing, dimensionless

NRe_G = Reynolds number for gas, $Dv\rho_G/\mu_G$, dimensionless

NRe_w = Reynolds number for liquid, $Dv\rho_w/\mu_w$, dimensionless

S = specific surface of the material, sq. ft./cu. ft.

S^2_θ = second central moment of the residence time distribution, sec.^{2}

t = time measured from introduction of signal, sec.

v = average superficial velocity, ft./sec.

V = volume of empty column, cu. ft.

q = volumetric flow rate through column, cu. ft./sec.

Greek Letters

ϵ = porosity of dry bed, volume fraction of empty column

ϵ_w = porosity of wet bed, volume fraction of empty column

ϵ_{wo} = coefficient for porosity correlation, dimensionless

θ = mean residence time $\epsilon V/q$ or L/v, sec.

μ_G = viscosity of gas lb./ft., hr.

μ_w = viscosity of the liquid lb./ft., hr.

ν = skewness, dimensionless third central moment of the distribution function

ρ_G = density of gas lb./cu. ft.

ρ_w = density of liquid, lb./cu. ft.

σ^2 = variance of the dimensionless time distribution function, dimensionless

LITERATURE CITED

1. Aris, Rutherford, and N. R. Amundson, *A.I.Ch.E. Journal*, 3, 280 (1957).
2. Carberry, J. J., and R. H. Bretton, *ibid.*, 4, 367 (1958).
3. Cohen, W. C., and E. F. Johnson, *Ind. Eng. Chem.*, 48, 1031 (1956).
4. Cramer, H., "The Elements of Probability Theory," Wiley, New York (1955).
5. Danckwerts, P. V., *A.I.Ch.E. Journal*, 1, 456 (1955).
6. ———, *Chem. Eng. Sci.*, 2, 1 (1953).
7. ———, J. W. Jenkins, and G. Place, *Chem. Eng. Sci.*, 3, 26 (1954).
8. Deisler, P. F., and R. H. Wilhelm, *Ind. Eng. Chem.*, 45, 1219 (1953).
9. Deisler, P. F., K. W. McHenry, and R. H. Wilhelm, *Anal. Chem.*, 27, 1366 (1955).
10. DeMaria, Francesco, Ph.D. thesis, Univ. Mich., Ann Arbor (May, 1958).
11. Ebach, E. A., and R. R. White, *A.I.Ch.E. Journal*, 4, 161 (1958).
12. Fellinger, L., ScD. thesis, Mass. Inst. Technol., Cambridge (1941).
13. Fowler, F. C., and G. G. Brown, *Trans. Am. Inst. Chem. Engrs.*, 39, 491 (1943).
14. Gilliland, E. R., and E. A. Mason, *Ind. Eng. Chem.*, 41, 1191 (1949).
15. *Ibid.*, 44, 218 (1952).
17. Jesser, B. W., and J. C. Elgin, *Trans. Am. Inst. Chem. Engrs.*, 34, 277 (1953).
18. Kramers, H., and G. Alberda, *Chem. Eng. Sci.*, 2, 173 (1953).
19. Klinkenberg, A., and F. Sjenitzer, *ibid.*, 5, 258 (1956).
20. Kozeny, J., *Ber. Wien. Akad.*, 136A, 271 (1925).
21. Lapidus, Leon, *Ind. Eng. Chem.*, 49, 1000 (1957).
22. Leva, Max, "Tower Packings and Packed Tower Design," U. S. Stoneware Company, Akron, Ohio (1953).
23. Levenspiel, O., and W. K. Smith, *Chem. Eng. Sci.*, 6, 227 (1957).
25. Mayo, F., T. G. Hunter, and A. W. Nash, *J. Soc. Chem. Ind. (London)*, 44, 375T (1935).
26. McHenry, K. W., Jr., and R. H. Wilhelm, *A.I.Ch.E. Journal*, 3, 83 (1957).
27. Sherwood, T. K., and R. L. Pigford, "Absorption and Extraction," McGraw-Hill, New York (1952).
28. Sherwood, T. K., G. H. Shipley, and F. A. L. Holloway, *Ind. Eng. Chem.*, 30, 765 (1938).
29. Singer, E., D. B. Todd, and V. P. Guin, *ibid.*, 49, 1 (1957).
30. Shulman, H. L., C. F. Ullrich, and N. Wells, *A.I.Ch.E. Journal*, 1, 247 (1955).
31. Spalding, D. B., *Chem. Eng. Sci.*, 3, 74 (1958).
32. van der Laan, E. Th., *ibid.*, 7, 187 (1958).
33. Whitt, F. R., *Brit. Chem. Eng.*, 1, 43 (1957).
34. Yagi, Sakae, and T. Miyauchi, *Chem. Eng. (Japan)*, 17, 382 (1953).

Manuscript received February 2, 1959; revision received December 18, 1959; paper accepted December 28, 1959. Paper presented at A.I.Ch.E. St. Paul meeting.